

# Thermoanalytical Study on the Crystallization and Transition of Nanoporous Anodic Alumina Membrane

Riko Ozao, Hirohisa Yoshida\*, Takeshi Inada\*\*, and Moyuru Ochiai

North Shore College of SONY Institute, Atsugi, Japan 243-8501

Fax: 81-46-247-3131, e-mail: ozao@ei.shohoku.ac.jp

\*Tokyo Metropolitan University, Hachi-oji, Tokyo, Japan, 192-0397

Fax: 81-426-77-2844, e-mail: yoshida-hirohisa@c.metro-u.ac.jp

\*\*Japan Fine Ceramics Center, Atsuta, Nagoya, Japan 456-8587

Fax: 81-52-871-3599, e-mail: inada@jfcc.or.jp

The morphological change at ca. 940 °C of anodically prepared alumina membrane and the influence of impurity carbon incorporated in the membrane structure on the transformation temperatures are studied. By detailed study using TMA and dilatometry in combination of simultaneous TG-DTA/FTIR, it is confirmed that carbon affects the kinetic reaction, i.e., dissociation of SO<sub>2</sub> at ca. 940 °C. The transformation temperature at ca. 1250 °C is influenced by the pore size, presumably due the critical crystallite (domain) size necessary to develop the stable  $\alpha$ -Al<sub>2</sub>O<sub>3</sub>. Furthermore, TEM observation revealed that alumina membranes maintain their pore structure to temperatures as high as 1200 °C.

Key words: mesopore, nanoporous membrane, TMA, simultaneous TG-DTA/FTIR, alumina polymorph

## 1. INTRODUCTION

Nanocrystalline powders have long attracted much attention because of their distinguished properties in processing novel materials [1]. On the other hand, nanoporous materials having pores ranging from 2 to 50 nm in diameter are referred to as mesoporous materials, and have been of particular interest because of their potential applicability to various fields such as catalyst supports, filters, electronic devices, luminescent devices, biological applications, templates, and various other functional material systems [2]. Well-known in the art are clay mesoporous structures [3], but most of them are prepared from silicates using pillaring reactions of lamellar solids, and less studies have been made on alumina materials.

Nanoporous alumina membranes having regularly arranged cylindrical hexagonal pores can be obtained by anodically oxidizing aluminum in oxalic acid, acetic acid, chromic acid, sulfuric acid, etc. [4]. Since the pore size of this material is fully controllable, nanoporous alumina membranes are promising concerning their applicability not only to various fields described above, but also as a standard material for use in the evaluation of thermal resistance [5]. Inada et al. [6] proposed a method of preparing anodic alumina membranes having controlled pore morphology for use as gas filters. The present authors have made studies on the thermal change of the anodically prepared amorphous alumina, and found that this material exhibits distinguished features on forming crystalline phases and in the subsequent polymorphic phase transformations [7, 8]. The nano- (or meso-) porous membrane above undergoes the final transformation to  $\alpha$ -Al<sub>2</sub>O<sub>3</sub> (i.e., the thermodynamically stable phase) at a temperature as

high as 1250 °C [8]. This is higher by 150 degrees or more than any of the transformation temperatures known heretofore. This signifies that the membrane retains its pores to temperatures as high as ca. 1250 °C. Furthermore, it has been found that the membrane shows a sharp exothermic reaction followed by an exothermic reaction, accompanied by a mass loss of about 8 %. However, from detailed studies using simultaneous TG-DTA/FTIR, it has been found that gaseous carbon dioxide is discharged at ca. 940 °C before discharging gaseous sulfur dioxide [7]. Since physically adsorbed gaseous species would not be retained to temperatures as high as 940 °C, the presence of gaseous carbon dioxide generated a novel question whether it influences the final transformation temperature.

The present study aims to investigate in detail the morphological change of the membrane at ca. 940 °C, and to investigate whether carbon has influence on the final transformation temperature of the membrane or not.

## 2. EXPERIMENTAL

### 2.1 Samples

An amorphous as-prepared alumina obtained by anodizing aluminum in sulfuric acid electrolyte described previously [7] was used in TMA and TEM observations. This sample, denoted 25, is about 150  $\mu$ m in thickness and has cylindrical pores about 25 nm in diameter. The as-prepared sample contains about 11 % by weight of SO<sub>2</sub> as determined by EDS [7].

New samples having pores with diameter 15 nm and 18 nm were prepared similarly as 25, except for changing the applied voltage to 15 V and 18 V, respectively.

Furthermore, decarbonated samples having pore sizes 15 nm, 18 nm, and 25 nm were newly prepared in the same manner as above, except for bubbling gaseous  $N_2$  into the electrolyte during anodization to avoid incorporation of carbon. The details of the samples are given in Table I below together with TG-DTA results.

## 2.2 TMA (thermomechanical analysis) and dilatometry

TMA was performed by using TMA4130S (manufactured by MAC Science Co., Ltd.) in a flow of gaseous  $N_2$  at a rate of  $200 \text{ ml min}^{-1}$  at a heating rate of  $20 \text{ deg min}^{-1}$  (from R.T. to  $600^\circ\text{C}$ ) and  $10 \text{ deg min}^{-1}$  (from  $600$  to  $1500^\circ\text{C}$ ), while applying load of  $10 \text{ g}$  against the planar surface of the sample  $150 \mu\text{m}$  in thickness. Sampling was made every  $1.0 \text{ sec}$ .

Isothermal measurement was made at  $940^\circ\text{C}$  by heating the sample to the temperature at a rate of  $10 \text{ deg min}^{-1}$ .

Dilatometry was performed on a sample fraction  $5.19 \text{ mm}$  in length by using TD5200S (manufactured by MAC Science Co., Ltd.) in a flow of gaseous  $N_2$  at a rate of  $200 \text{ ml min}^{-1}$  at a heating rate of  $20 \text{ deg min}^{-1}$  (from R.T. to  $600^\circ\text{C}$ ) and  $10 \text{ deg min}^{-1}$  (from  $600$  to  $1500^\circ\text{C}$ ).

## 2.3 TEM observation

For TEM observation, samples were prepared in the following manner. Sample fractions were each subjected to size reduction. A micromesh (i.e., a 3-dimensionally woven special polymer) was placed on a copper grid to fix the size-reduced sample, and the grid was reversed for carbon coating. TEM observation was carried out by using JEOL transmission microscope model JEOL 2000FX.

## 2.4 Simultaneous TG-DTA/FTIR

The simultaneous system consists of a TG-DTA 6200 module of Seiko SSC5200II TA system (Seiko Instruments, Inc) connected to a JASCO FT/IR-620 Fourier-transform infrared spectrometer equipped with a MCT (Mercury Cadmium Telluride) detector. This allows a high sensitivity run with a resolution of  $2 \text{ cm}^{-1}$  in single scan. A 1/16-inch stainless steel tube was used to connect the TG-DTA module and the FT-IR spectrometer system, and the system was optimized in such a manner that the gas evolved from the sample placed in the TG-DTA furnace may reach the FT-IR cell within 1 second. Thus, sampling was made every 14 seconds. Gaseous  $N_2$  was flown as a carrier gas at the optimized flow rate of  $175 \text{ ml min}^{-1}$ . Scanning was made in a temperature range of  $30 - 1400^\circ\text{C}$ .

## 2.5 High-temperature simultaneous TG-DTA

High temperature simultaneous TG-DTA was performed on ca.  $5 \text{ mg}$  of sample placed in a Pt pan inside a vertical type furnace of TG-DTA 2200 (R.T.- $1700^\circ\text{C}$ ) manufactured by MAC Science Co. Ltd. Gaseous  $N_2$  was flown at a rate of  $100 \text{ ml min}^{-1}$ . The sample was heated at a rate of  $20 \text{ deg min}^{-1}$ .

## 3. RESULTS AND DISCUSSION

### 3.1 TMA and dilatometry

Figure 1 shows the average expansion coefficient of sample 25 (non-treated sample with 25-nm diameter pores, see Table 1) obtained by TMA and DLT, together with the corresponding TG-DTA curves. It can be understood that the sample contracts anisotropically in the direction perpendicular to the plane of the membrane up to the exothermic-endothermic reaction, but that it thereafter contracts isotropically ascribed to the gradual formation of polycrystals. Since the average linear expansion coefficient of  $\alpha$ -alumina is  $0.80 (\times 10^{-5} / \text{K})$ , the phase present is not purely crystalline, but suggests the presence of quasi-crystals, or the presence of numerous pores. This may be evidence of the inaccessible pores or fissures as pointed out by Patch et al. [9].

Fig. 1 Average Linear expansion coefficient values superposed on TG-DTA.

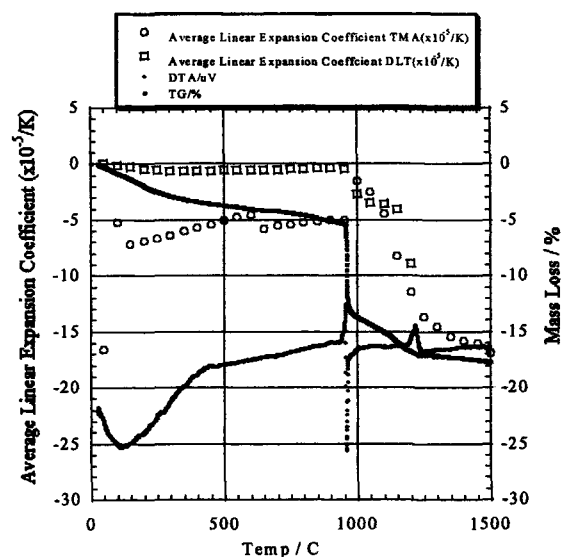
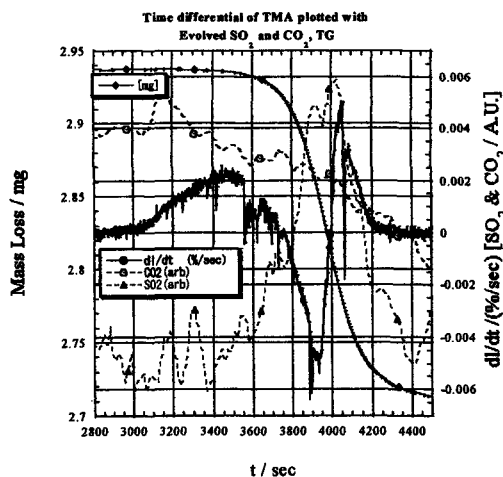


Fig. 2 Time differential of TMA at  $940^\circ\text{C}$ .



Further, Fig. 2 shows the results obtained by holding TMA isothermally at 940 °C, in which simultaneous TG-DTA/FTIR results are superposed. The time differential of TMA shows that the change here should be considered kinetically, and it suggests that the expansion and contraction are closely related with gas evolution. Although an attempt was made for kinetic analysis, this reaction could not be fitted to any nucleation-growth mechanism or any other reaction processes. Hence, the expansion and contraction may be a consequence of synergetically occurring various reactions such as diffusion, nucleation, gas expansion, desorption, and the destruction of the micropores.

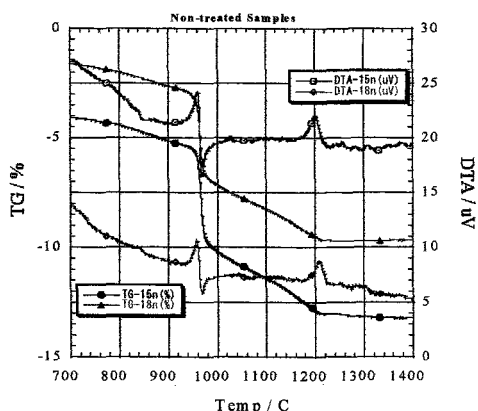
3.2 Simultaneous TG-DTA/FTIR and high temperature TG-DTA of decarbonated samples

Table I shows the TG-DTA results of the samples. In Fig. 3 are given the TG-DTA curves (700-1400°C) of the newly prepared non-treated samples (having 15-nm and 18-nm diameter pores). In case of non-treated samples, it can be understood that the 1<sup>st</sup> Ex-En peak temperature is less influenced by the pore diameter, but that the second Ex peak temperature clearly shifts to the lower side with decreasing pore size.

Table I Details of the samples

Pore diameter / nm	Theoretical SO <sub>2</sub> / %	Found SO <sub>2</sub> / %	Peak Temperature / °C		
			1 <sup>st</sup> DTA Ex	1 <sup>st</sup> DTA En	2 <sup>nd</sup> DTA Ex
Decarbonated					
15	8.02	8.0	958	971	1208
18	8.95	9.0	960	968	1215
25	11.14	11.0	970	975	1230
Nontreated					
15	8.02	8.0	960	970	1200
18	8.95	9.0	960	970	1209
25	11.14	11.0	974	976	1240

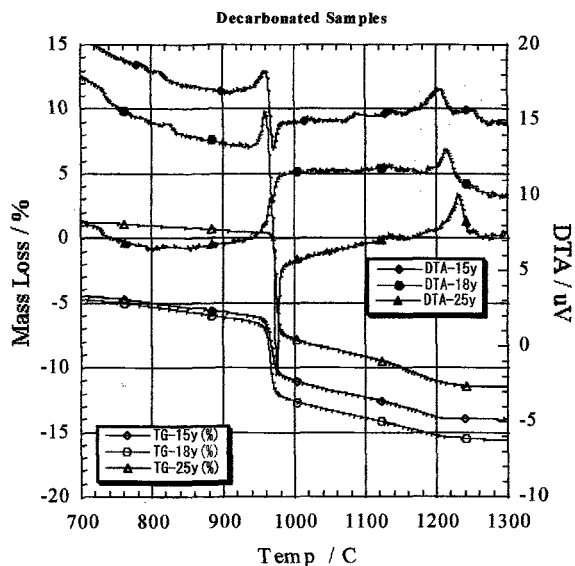
Fig. 3 TG-DTA of samples containing carbon.



In Fig. 4 are shown the TG-DTA results (700-1300°C) of the newly prepared decarbonated samples (15, 18, 25 nm diameter pores). It can be understood from these results that the first Ex-En peak and the second Ex peak temperatures are both influenced by the pore diameter. That is, the temperatures shift to the lower side with decreasing pore diameter.

Referring to the case of decarbonated samples shown in Fig. 4, the 1<sup>st</sup> Ex-En temperature is slightly influenced by the pore size. Furthermore, the first mass loss is

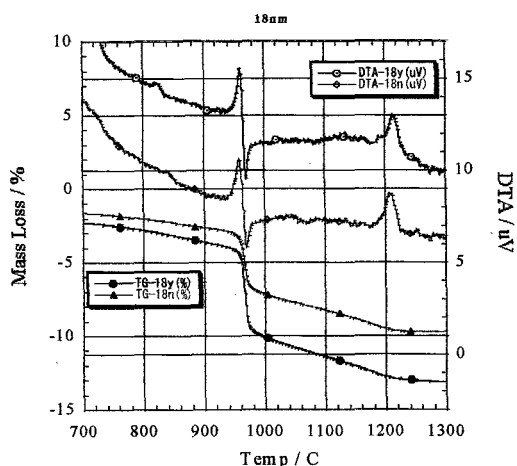
Fig. 4 TG-DTA of decarbonated samples.



greater with increasing pore size, i.e., with the increasing total SO<sub>2</sub> content. By taking the results above for non-treated samples in consideration, presumably, discharge of carbon dioxide, which is incorporated as an impurity, takes time to initiate the fundamental reaction of discharging SO<sub>2</sub>.

The total mass loss up to ca. 1200°C is roughly in correspondence with the total SO<sub>2</sub> content obtained by TEM EDS. Thus, it can be understood that sulfate ions incorporated into the pore walls are not completely discharged in the first Ex-En. Furthermore, particularly in the non-treated samples, the mass loss in the first Ex-En is not in conformity with the theoretical SO<sub>2</sub> content. Since the first Ex-En corresponds to the crystallization into quasi-crystalline phase consisting of alumina polymorphs of minute domain size observed as ring patterns by TEM diffraction, this evidences that the crystallization

Fig. 5 Comparison of TG-DTA for 18-nm pore samples (decarbonated and non-treated).



occurs depending on temperature without requiring sufficient development of domain size.

This is shown more clearly in Fig. 5, in which 18-nm pore samples are compared. The curves shown by 18y are the decarbonated sample, and 18n show the non-treated sample. The mass loss is greater for the 18y sample, showing that the presence of carbon somewhat hinders the dissociation of  $\text{SO}_2$ .

Fig. 6 FTIR spectra of discharged gas species.

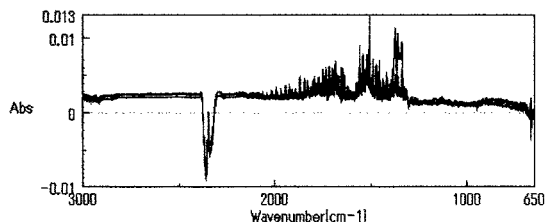


Fig. 7 Change in FTIR intensity of  $\text{SO}_2$  with time.

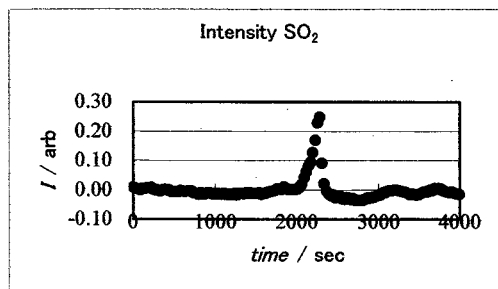


Figure 6 shows the discharged gas species obtained by simultaneous TG-DTA/FTIR. In the figure are superposed the spectra obtained at ca. 915, 950, and 970 °C. The ordinate is shown by intensity ratio (arbitrary) with respect to the spectrum obtained at R.T. Since at the initial spectrum obtained at R.T. shows presence of  $\text{CO}_2$  in ambient, the reversed band at ca.  $2400\text{ cm}^{-1}$  shows that the sample discharges no  $\text{CO}_2$  in the sampled temperatures. The fine bands at ca.  $1600\text{ cm}^{-1}$  show presence of  $\text{H}_2\text{O}$  molecules. The sharp band at ca.  $1370\text{ cm}^{-1}$  and the slight band at ca.  $1160\text{ cm}^{-1}$ , which are obtained only at 950 °C, correspond to the SO asymmetric stretching vibration and symmetric stretching vibration for gaseous  $\text{SO}_2$ , respectively. It is therefore confirmed that the decarbonated samples are completely free from  $\text{CO}_2$ .

Figure 7 shows the change in intensity (arbitrary unit) of gaseous  $\text{SO}_2$  band at ca.  $1370\text{ cm}^{-1}$  with elevating temperature. It can be seen that  $\text{SO}_2$  is discharged quickly at ca. 950 °C, but that the discharge of gaseous  $\text{SO}_2$  still continues to higher temperatures. This result is in conformity with the TG loss.

Thus, by taking the above results into consideration, the gradual mass loss which takes place after the 1<sup>st</sup> Ex-En corresponds to the gradual discharge of  $\text{SO}_2$  necessary for the formation of the alumina polymorph crystallites, and for the growth of crystallites to the critical size. According to Wen and Yen [10], the

nucleation of  $\alpha\text{-Al}_2\text{O}_3$  initiates only when  $\theta\text{-Al}_2\text{O}_3$  reaches a critical size of 17 nm. However, in the present study,  $\gamma\text{-Al}_2\text{O}_3$  was still confirmed to be present at 1100 °C. Furthermore, the transformation to  $\alpha\text{-Al}_2\text{O}_3$  in the present study occurs at higher temperatures with increasing pore size. Since the wall thickness is approximately double the pore diameter, the samples 15, 18, and 25 studied herein can be roughly considered to consist of columns 30 nm, 36 nm, and 50 nm in width. Since the final transformation occurs only after complete mass loss (i.e., at which TG shows plateau at ca. 1100 °C or higher temperature), the transformation in this case may occur in a somewhat oriented manner. Hence, the thinner the wall is, the higher the mobility would become for the dissociation of gaseous  $\text{SO}_2$ . In addition, the present sample was found to contain water. Most of them are lost at temperatures below 500 °C as zeolitic water, but OH groups are presumably present to temperatures as high as 1100 °C. Further study on them is under way.

## CONCLUSIONS

The morphological change at ca. 940 °C of anodically obtained alumina membrane and the influence of impurity carbon incorporated in the membrane structure on the transformation temperatures were studied mainly by high temperature TG-DTA. By detailed study of TMA and dilatometry in combination of simultaneous TG-DTA/FTIR, it is confirmed that carbon affects the kinetic reaction, i.e., dissociation of  $\text{SO}_2$  at ca. 940 °C. The transformation temperature at ca. 1250 °C is influenced by the pore size, presumably due the critical crystallite (domain) size necessary to develop the stable  $\alpha\text{-Al}_2\text{O}_3$ . Furthermore, TEM observation revealed that alumina membranes maintain their pore structure to temperatures as high as 1200 °C.

## ACKNOWLEDGEMENTS

The authors are grateful to Ms. K. Kajiyama of MAC Science, who aided us with TMA and high temperature TG-DTA measurements.

## REFERENCES

- [1] H. Gleiter, *Prog. Mater. Sci.*, **33**, 223 (1989).
- [2] See, for example, K. Kuroda, *Bull. Cer. Soc. Jpn.*, **36**, 902 (2001) (In Japanese).
- [3] A. Galarneau et al., *Nature*, **374**, 529 (1995).
- [4] R.C. Furneaux, W.G. Rigby and A.P. Davidson, *Nature*, **337**, 147 (1989).
- [5] R. Ozao, M. Ochiai, H. Yoshida, Y. Ichimura and T. Inada, *Thermochim. Acta*, **352-353**, 91 (2000).
- [6] T. Inada and T. Fukui, *Proc. 13<sup>th</sup> Korea-Japan Seminar on New Ceramics*, p. 340 (1996).
- [7] R. Ozao, H. Yoshida, Y. Ichimura, T. Inada and M. Ochiai, *J. Therm. Anal. Cal.*, **64**, 915 (2001).
- [8] R. Ozao, M. Ochiai, H. Yoshida, Y. Ichimura and T. Inada, *J. Therm. Anal. Cal.*, **64**, 923 (2001).
- [9] L. Patch, R. Roy, S. Komarnei, *J. Mater. Res.*, **5**, 278 (1990).
- [10] H-L. Wen and F-S. Yen, *J. Crystal Growth*, **208**, 696 (2000).